Electronic Supplementary Material (ESI) for Dalton Transactions.

Supporting Information for

Electrocatalytic Generation of H_2 from Neutral Water in Acetonitrile Using Manganese Polypyridyl Complexes with Ligand Assistance

Gyandshwar Kumar Rao, Mohammad Parsa Jamshidi, Jeremy I. G. Dawkins, Wendy Pell, Illia Korobkov, Darrin Richeson*

Department of Chemistry and Biomolecular Sciences and the Center for Catalysis Research and Innovation, University of Ottawa, Ottawa, Ontario K1N6N5

Content **Pages**

Experimental:

General Procedures. Reagents and analytical grade solvents were purchased from Strem Chemicals or Sigma Aldrich and used without further purification. Tris-2-picolylamine or tris(2-pyridylmethyl)amine (tpa) was prepared according to the literature procedure (Britovesk, G. J. P; England, J; White A. J. P; *Inorg.Chem.* **2005**, 44, 8125). The ^{1}H, ^{13}C{^{1}H} and ^{19}F{^{1}H} NMR spectra were recorded at 400, 100 and 376 MHz respectively with chemical shifts reported in ppm using the residual protons of the NMR solvent as internal standards. Carbon-13 DEPT NMR experiments were used routinely to determine the number of hydrogen atoms linked to carbon atoms. IR spectra were collected using an Agilent Cary FTIR spectrometer.

Electrochemical experiments have been carried out in a single compartment cell wrapped with aluminum foil using a VersaSTAT 3 (Princeton Applied Research) potentiostat. Samples were prepared in a glovebox, sealed, removed from the glovebox and connected to a Schlenk line and maintained under a nitrogen atmosphere. A conventional three electrode system was employed consisting of a glassy carbon working electrode (diameter = 0.2 cm), a Pt wire as the auxiliary electrode, and an Ag wire as a pseudo-reference electrode. Ferrocene was added as a reference compound. Dried acetonitrile was purchased from Sigma Aldrich and stored on molecular sieves in glove-box. Tetrabutylammoniumhexafluorophosphate, $[(n\text{-}Bu)_4N]PF_6$ (TBAHFP), the supporting electrolyte, was crystallized two times with methanol, dried in vacuum at 90 °C for 24 h before used and stored in a glovebox. The electrolyte solution, 0.1 M $[(n\text{-}Bu)_4N]PF_6$ in CH_3CN, was saturated with N_2 by purging with N_2 for 10 min prior to each experiment. The concentration of catalyst was 1 mM (15 mL acetonitrile) in each experiment. For bulk electrolysis experiments the working electrode was a glassy carbon rod (diameter = 0.4 cm; length 2 cm) with Pt gauze as the auxiliary electrode and a Ag wire as pseudo-reference electrode. Water or aqueous phosphate buffer was added to the electrolyte solution as the source of hydrogen. Hydrogen production was measured using an Agilent 7820A gas chromatograph (GC) with an Agilent select permanent gases column and equipped with a thermal conductivity detector (TCD). Mass spectra measurements were carried out in an Agilent 5977E GC/MSD using a DB-5ms column.

X-ray Crystallography: The crystals were mounted on thin glass fibers using paraffin oil. Prior to data collection crystals were cooled to 200.15 °K. Data were collected on a Bruker AXS SMART single crystal diffractometer equipped with a sealed Mo tube source (wavelength 0.71073 Å) APEX II CCD detector. Raw data collection and processing were performed with APEX II software package from BRUKER AXS.[1] Initial unit cell parameters were determined from 60 data frames with 0.3° ω scan each collected at the different sections of the Ewald sphere. Semi-empirical absorption corrections based on equivalent reflections were applied.[2] Systematic absences in the diffraction data-set and unit-cell parameters were consistent with the assigned space group. The structures were solved by direct methods, completed with difference Fourier synthesis, and refined with full-matrix least-squares procedures based on F^2. All hydrogen atoms positions were calculated based on the geometry of the related non-hydrogen atoms. All hydrogen atoms were treated as idealized contributions during the refinement. All scattering factors are contained in several versions of the SHELXTL program library, with the latest version used being v.6.12.[3]

Computational Details: Optimized structures were obtained from density functional theory (DFT) computations using Gaussian 09.[4] Computations were performed on complexes solvated with acetonitrile using the integral equation formalism variant of PCM, with the default parameters for acetonitrile. The TZVP basis set was used for all atoms. Using the optimized starting structure for $[Mn(\kappa^3\text{-tpa})(CO)_3]^+$ (**1**$^+$), further optimized structures were determined for the single and double reduction products, $[Mn(\kappa^3\text{-tpa})(CO)_3]$ (**1**) and $[Mn(\kappa^3\text{-tpa})(CO)_3]^-$ (**1**$^-$**)**, in acetonitrile. Protonation of each of these species was explored computationally by locating the added protons in various locations within the reduced species followed by re-optimization. All of these optimizations were performed in acetonitrile. In the case of the singly reduced complex, $[Mn(\kappa^3\text{-tpa})(CO)_3]$ (**1**), the lowest energy structure was observed for protonation of uncoordinated py, $[Mn(\kappa^3\text{-tpaH})(CO)_3]^+$(**1H)** as represented in Fig. S23 and Table S10. Using a similar procedure, the lowest energy optimized structure of the protonation of the doubly reduced species $[Mn(\kappa^3\text{-tpa})(CO)_3]^-$ (**1**$^-$**)**, was observed to be $[MnH(\kappa^3\text{-tpa})(CO)_3]$ (**1**$^-$**H**) and these results are represented in Fig S24 and Table S11. Addition of a second proton to this protonated

doubly reduced species, **1**$^{-}$**H**, was explored and the lowest energy optimized structure was determined to be [MnH(κ^3-tpaH)(CO)$_3$]$^+$(**1**$^{-}$**HH**$^+$) with results presented in Fig. S25 and Table S12.

Synthesis of [Mn(κ^3-tpa)(CO)$_3$]Br (1$^+$Br$^-$**)**. A solution of tpa ligand (0.298 g, 1mmol) was prepared in 15 mL of tetrahydrofuran in a nitrogen glovebox. To this stirred solution was addedMn(CO)$_5$Br (0.274 g, 1mmol) . The flask was removed from the glovebox and attached to a Schlenk line, wrapped with aluminum foil and heated 80 °C under $N_2$for 2 h. The solution was cooled and the volume was reduced to ~10 mL *in vacuo*. The resulting yellow precipitate was removed by filtration to give complex **1**$^+$Br$^-$. Compound **1**$^+$Br$^-$ was crystallized from a saturated dichloromethane solution via slow diffusion of hexane. Yield 0.425 g (82%).^{1}H (DMSO-d_6, 400MHz): δ 8.89 (d, 2H, ^3J = 5.6 Hz), 8.74 (dd, 1H, ^3J, ^3J = 4Hz, 5.6 Hz), 7.98-8.02 (m, 1H), 7.86-7.92 (m, 3H), 7.52-7.56 (m, 1H), 7.42-7.48 (m, 4H), 5.27 (d, 2H, ^2J = 17.2 Hz), 4.96 (s, 2H), 4.39 (d, 2H, ^2J = 17.2 Hz). ^{13}C {^{1}H} (DMSO-d_6, 100MHz): δ 218.6 (br), 160.9, 153.8, 152.5, 149.9, 140.0, 137.9, 126.8, 125.8, 124.6, 123.2, 71.7, 67.6. IR (cm^{-1}): 3105, 2032, 1914, 1906, 1604, 1586, 1570, 1477, 1427, 1366, 1296, 1256, 1145, 1099, 1059, 1049, 1010, 994, 967, 923, 901, 881, 842, 780, 772, 717, 691, 651, 626, 548. HR-MS (CH_3CN): [M]$^+$*m/z* 429.0773; calcd value for $C_{21}H_{18}N_4O_3Mn$ 429.0759 (δ = 3.2ppm).

Synthesis of [Mn(κ^3-tpa)(CO)$_3$]OTf (**1**$^+$OTf$^-$). A solution of complex **1**$^+$Br$^-$ (0.259 g, 0.5 mmol) was prepared in 10 mL of dichloromethane in a nitrogen glovebox. To this stirring solution was added silver trifluoromethanesulphonate (AgOTf) (0.128 g, 0.5 mmol) . The flask was wrapped with aluminum foil and stirred at room temperature for an additional 16 h under N_2. The solution was filtered and solvent was removed *in vacuo* to give a yellow solid. Single crystals of **1**$^+$OTf$^-$ were grown by slow diffusion of hexane into a saturated dichloromethane solution. Yield 0.326 g (84%).^{1}H (DMSO-d_6, 400MHz): δ 8.86 (d, 2H, ^3J = 5.2 Hz), 8.71 (d, 1H, ^3J = 4 Hz), 7.94-7.98 (m, 1H), 7.80-7.87 (m, 3H), 7.49-7.52 (m, 1H), 7.37-7.43 (m, 4H), 5.22 (d, 2H, ^2J = 17.2 Hz), 4.92 (s, 2H), 4.34 (d, 2H, ^2J = 17.2 Hz). ^{13}C{^{1}H}(DMSO-d_6, 100MHz): δ 218.4 (br), 160.9, 153.8, 152.5, 149.9, 140.0, 137.9, 126.7, 125.8, 123.1, 122.7,123.2,71.8, 67.9. ^{19}F (DMSO-d_6, 376.7MHz): δ −77.7. IR (ATR, cm^{-1}): 2029, 1913, 1906, 1606, 1587, 1570, 1477, 1425, 1368, 1294, 1256, 1140, 1099, 1069, 1049, 1010, 994, 924, 900, 885, 843, 780, 772, 716, 690, 651,

623. HR-MS (CH_3CN): $[M]^+$*m/z* 429.0773; calcd value for $C_{21}H_{18}N_4O_3Mn$ 429.0795 (δ = 5.1 ppm).

Synthesis of [Re(κ^3-tpa)$(CO)_3$]Cl (**2**$^+$$Cl^-$). A solution of tpa ligand (0.145 g, 0.487mmol) was made in 15 mL of tetrahydrofuran in a nitrogen glovebox. To this stirring solution was added $Re(CO)_5Cl$ (0.150 g, 0.415mmol). The flask removed from the glovebox, connected to a Schlenk line and heated to 80°C and stirred for an additional 2h under N_2. The solution was cooled and the volume was reduced to ~10 mL *in vacuo*. The resulting colorless precipitate of **2**$^+$$Cl^-$ was isolated by filtration. Single crystals of **2**$^+$$Cl^-$ were grown by slow diffusion of hexane into a saturated chloroform solution. Yield 0.2299 g (93%). ^{1}H (DMSO-d_6, 400MHz): δ 8.80 (d, 2H, ^3J = 5.6 Hz), 8.71-8.73 (m, 1H), 7.97-8.02 (m, 3H), 7.83 (d, 1H, ^3J = 8.0Hz), 7.59-7.52 (m, 3H), 7.42-7.37 (m, 2H), 5.37 (d, 2H, ^2J = 16.8 Hz), 4.97 (s, 2H), 4.75 (d, 2H, ^2J = 16.8 Hz). ^{13}C (DMSO-d_6, 400MHz): δ 196.0, 195.2, 160.5, 153.7, 151.7, 149.4, 140.5, 137.4, 126.8, 125.4, 124.6, 123.1, 71.9, 68.1. IR (ATR, cm^{-1}): 2025, 1937, 1896, 1608, 1588, 1571, 1484, 1465, 1281, 1058, 991, 935, 773, 761, 735, 660, 642, 623, 546, 537. HR-MS (CH_3CN): $[M]^+$*m/z* 559.0815; calcd value for $C_{21}H_{18}N_4O_3Re$ 559.0836 (δ = -3.7 ppm).

Synthesis of [Re(κ^3-tpa)$(CO)_3$]OTf (**2**$^+$$OTf^-$). A solution of complex **2**$^+$$Cl^-$ (0.0403 g, 0.0626mmol) was prepared in 20 mL of dichloromethane in a nitrogen glovebox. To this stirring solution was added silver trifluoromethanesulphonate (AgOTf) (0.0162 g, 0.0626mmol). The flask was wrapped with aluminum foil and stirred at room temperature for an additional 30 min. The solution was filtered and solvent was removed *in vacuo* to give a colorless solid. Single crystals of **2**$^+$$OTf^-$ were grown by slow diffusion of pentane into a saturated dichloromethane solution. Yield: 0.0340g (77%). ^{1}H (DMSO-d_6, 300MHz): δ 8.81 (d, 2H, ^3J = 5.4Hz), 8.74-8.72 (m, 1H), 8.03-7.94 (m, 3H), 7.80 (d, 1H, ^3J = 7.5Hz), 7.57-7.52 (m, 3H), 7.42-7.37 (m, 2H), 5.37 (d, 2H, ^2J = 16.5Hz), 4.97 (s, 2H), 4.71 (d, 2H, ^2J = 16.5Hz). ^{13}C (DMSO-d_6, 300MHz): δ 196.0, 195.2, 160.6, 153.8, 151.8, 149.4, 140.5, 137.5, 126.5, 125.6, 124.3, 123.5, 122.8(q), 72.0, 68.1. ^{19}F (DMSO-d_6, 282MHz): δ −77.6. IR (ATR, cm^{-1}): 2029, 1909, 1612, 1591, 1448, 1275, 1257, 1222, 1151, 1030, 962, 914, 832, 765, 750, 636, 573, 548. HR-MS (CH_3CN): $[M]^+$*m/z* 559.0972; calcd value for $C_{21}H_{18}N_4O_3Re$ 559.0909 (δ = 11.3ppm).

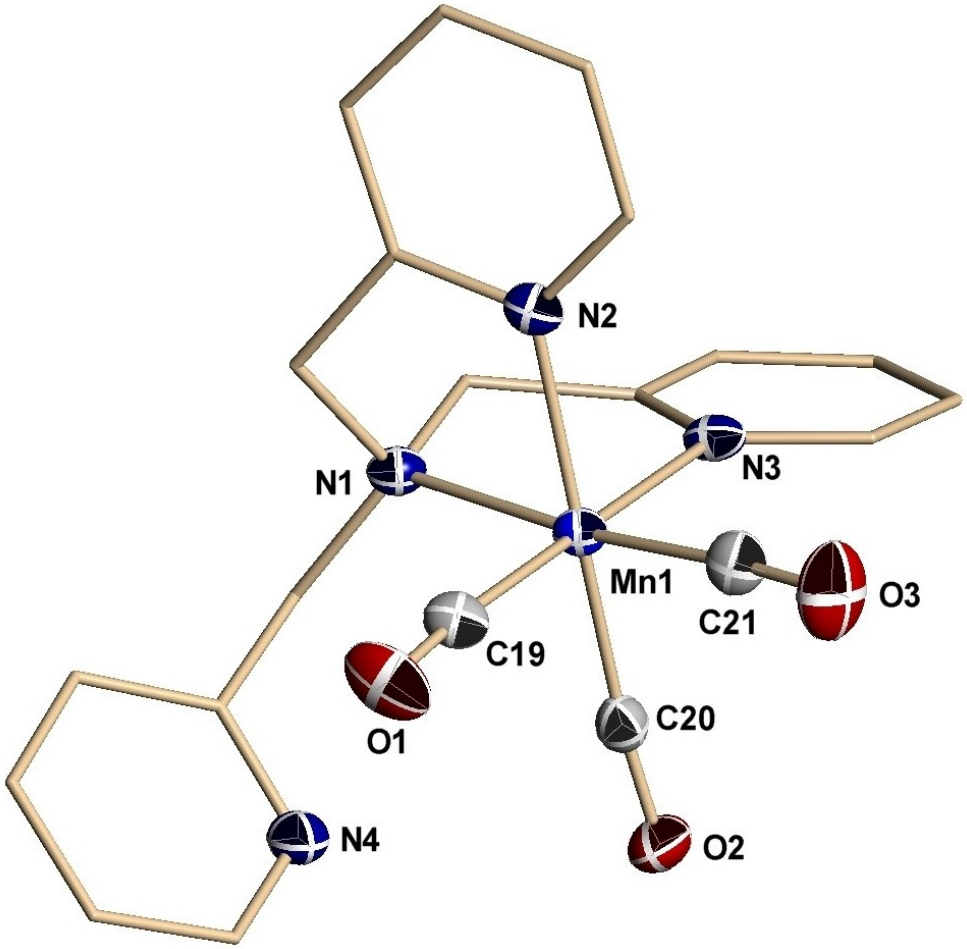

Figure S1. Structural representation of the cation component of the complex [Mn([κ³-tpa)(CO)$_3$]Br (**1**$^+$Br$^-$). Hydrogen atoms and the thermal ellipsoids of the ligand carbon atoms and the bromide anion are omitted for clarity.

Table S1. Single crystal X-ray structure parameters for compounds **2**$^{+}$Cl^{-}and **2**$^{+}$OTf^{-}.

Compound	[Re(κ^3-tpa)(CO)$_3$]Cl, **2**$^{+}$Cl^{-}	[Re(κ^3-tpa)(CO)$_3$]OTf, **2**$^{+}$OTf^{-}
Empirical formula	$C_{21}H_{18}Cl_1N_4O_3Re(CHCl_3)(H_2O)$	$(C_{22}H_{18}F_3N_4O_6ReS)_2(H_2O)$
Formula weight	733.43	1437.34
Temperature (K)	200(2)	200(2)
λ(Å)	0.71073	0.71073
Crystal system	Triclinic	Orthorhombic
Space group	P -1	P 2_12_12
a (Å)	10.758(3)	16.8249(14)
b (Å)	10.896(3)	24.919(2)
c (Å)	11.559(3)	12.1149(10)
α (deg)	85.079(14)	90
β (deg)	81.257(15)	90
γ (deg)	83.576(15)	90
V (Å^3)	1327.4(7)	5079.2(7)
Z	2	4
ρ (calc) (Mg/m^3)	1.835	1.880
μ (mm^{-1})	5.015	4.936
Absorption correction	Semi-empirical from equivalents	
Final R indices [I>2σ(I)]		
R1[a]	0.0223	0.0248
*w*R2[b]	0.0537	0.0545

Table S2. Select bond lengths (Å) and angles (deg) from the single crystal X-ray analysis for complexes **2**$^{+}$Cl^{-}and **2**$^{+}$OTf^{-}.

[Re(κ^3-tpa)(CO)$_3$]Cl, **2**$^{+}$Cl^{-}		[Re(κ^3-tpa)(CO)$_3$]OTf, **2**$^{+}$OTf^{-}			
Re(1)-C(19)	1.907(4)	Re(1)-C(20)	1.927(6)		
Re(1)-C(21)	1.916(3)	Re(1)-C(19)	1.933(7)		
Re(1)-C(20)	1.928(3)	Re(1)-C(21)	1.941(6)		
Re(1)-N(2)	2.173(2)	Re(1)-N(3)	2.175(5)		
Re(1)-N(3)	2.175(3)	Re(1)-N(2)	2.187(5)		
Re(1)-N(1)	2.224(3)	Re(1)-N(1)	2.249(5)		
O(1)-C(19)	1.150(4)	Re(2)-C(40)	1.911(7)		
O(2)-C(20)	1.145(3)	Re(2)-C(41)	1.915(6)		
O(3)-C(21)	1.163(4)	Re(2)-C(42)	1.917(7)		
		Re(2)-N(7)	2.164(5)		
		Re(2)-N(6)	2.177(5)		
		Re(2)-N(5)	2.222(5)		
		O(1)-C(19)	1.142(8)		
		O(2)-C(20)	1.145(7)		
		O(3)-C(21)	1.135(7)		
		O(4)-C(40)	1.166(8)		
		O(5)-C(41)	1.158(7)		
		O(6)-C(42)	1.158(7)		
C(19)-Re(1)-C(21)	89.37(14)	C(20)-Re(1)-C(19)	85.8(3)	C(41)-Re(2)-N(6)	171.9(2)
C(19)-Re(1)-C(20)	87.82(13)	C(20)-Re(1)-C(21)	88.5(2)	C(42)-Re(2)-N(6)	96.3(2)
C(21)-Re(1)-C(20)	90.82(13)	C(19)-Re(1)-C(21)	86.4(3)	N(7)-Re(2)-N(6)	78.78(18)
C(19)-Re(1)-N(2)	94.99(11)	C(20)-Re(1)-N(3)	94.6(2)	C(40)-Re(2)-N(5)	174.8(2)
C(21)-Re(1)-N(2)	96.11(10)	C(19)-Re(1)-N(3)	98.5(2)	C(41)-Re(2)-N(5)	95.3(2)
C(20)-Re(1)-N(2)	172.54(12)	C(21)-Re(1)-N(3)	174.3(2)	C(42)-Re(2)-N(5)	97.5(2)
C(19)-Re(1)-N(3)	96.64(12)	C(20)-Re(1)-N(2)	172.0(2)	N(7)-Re(2)-N(5)	78.37(17)
C(21)-Re(1)-N(3)	173.55(11)	C(19)-Re(1)-N(2)	99.0(2)	N(6)-Re(2)-N(5)	77.62(19)
C(20)-Re(1)-N(3)	91.76(12)	C(21)-Re(1)-N(2)	98.18(19)		
N(2)-Re(1)-N(3)	81.06(9)	N(3)-Re(1)-N(2)	78.42(17)		
C(19)-Re(1)-N(1)	172.36(10)	C(20)-Re(1)-N(1)	97.0(2)		
C(21)-Re(1)-N(1)	95.28(12)	C(19)-Re(1)-N(1)	175.4(2)		
C(20)-Re(1)-N(1)	98.15(11)	C(21)-Re(1)-N(1)	97.3(2)		
N(2)-Re(1)-N(1)	78.51(9)	N(3)-Re(1)-N(1)	77.60(18)		
N(3)-Re(1)-N(1)	78.50(9)	N(2)-Re(1)-N(1)	77.86(17)		
		C(40)-Re(2)-C(41)	87.6(3)		
		C(40)-Re(2)-C(42)	86.8(3)		
		C(41)-Re(2)-C(42)	88.5(2)		
		C(40)-Re(2)-N(7)	97.2(2)		
		C(41)-Re(2)-N(7)	96.0(2)		
		C(42)-Re(2)-N(7)	174.1(2)		
		C(40)-Re(2)-N(6)	99.1(2)		

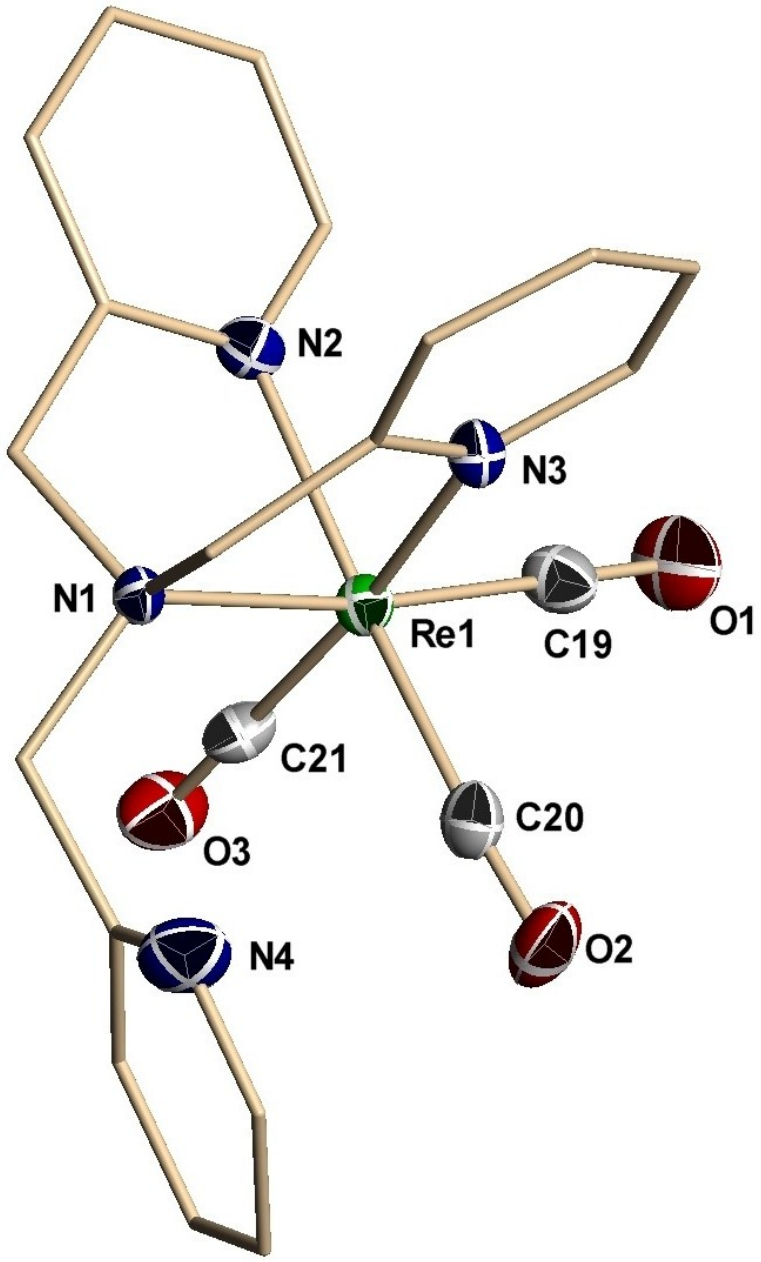

Figure S2. Structural representation of the cation component of the complex [Re([κ^3- tpa)$(CO)_3$]Cl (**2**$^+$Cl$^-$). Hydrogen atoms, the thermal ellipsoids of the ligand carbon atoms, chloride anion and co-crystallized chloroform and water are omitted for clarity.

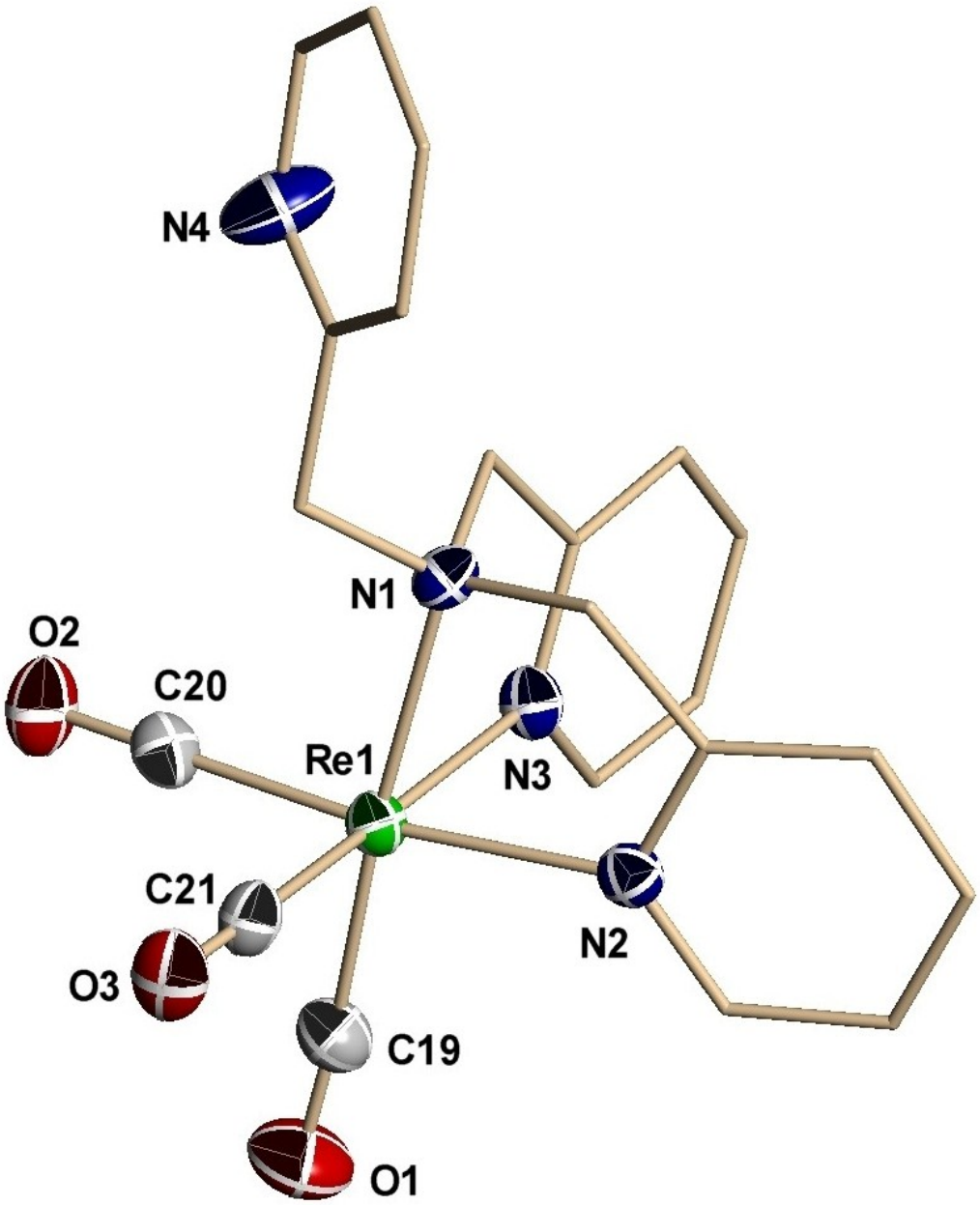

Figure S3. Structural representation of one of the two cations observed in the crystal structure of complex [Re([κ^3- tpa)$(CO)_3$]OTf (**2**$^+$OTf$^-$). Hydrogen atoms, the thermal ellipsoids of the ligand carbon atoms, triflate anion and co-crystallized water are omitted for clarity.

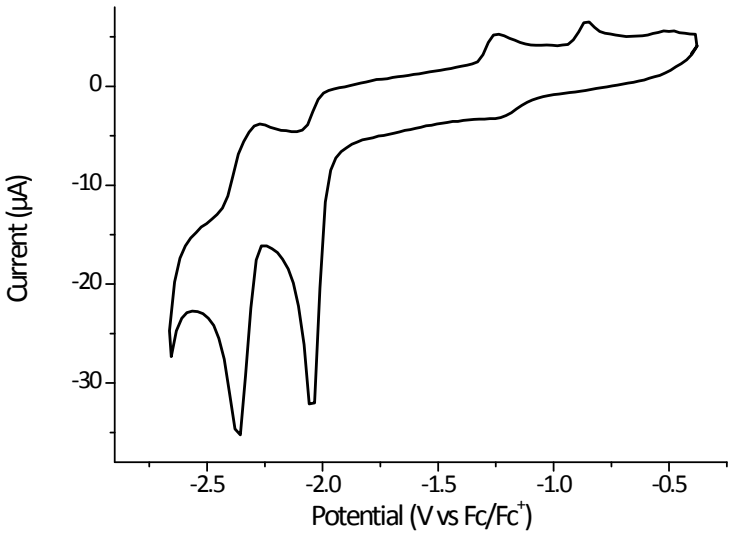

Figure S4. Cyclic voltammogram of [Mn(κ^3-tpa)$(CO)_3$]OTf under N_2 in CH_3CN with 0.1M tetrabutylammoniumhexafluorophosphate (TBAHFP) supporting electrolyte at 100 mV/s.

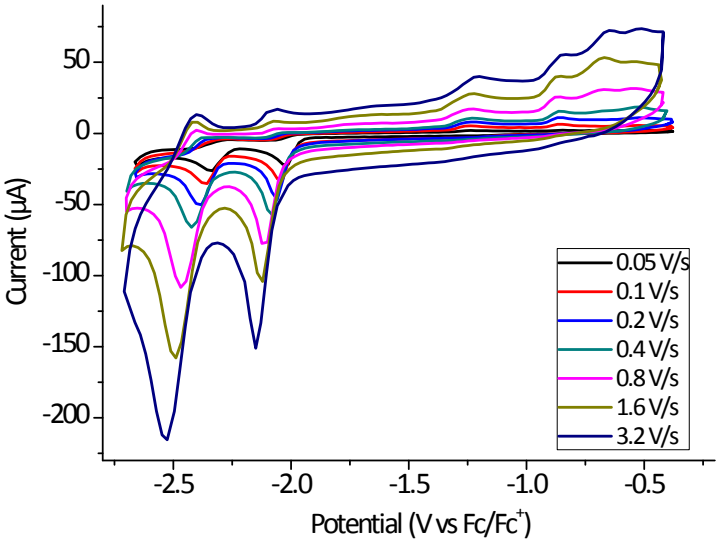

Figure S5. Cyclic voltammogram of [Mn(κ^3-tpa)$(CO)_3$]OTf in CH_3CN with 0.1M tetrabutylammoniumhexafluorophosphate (TBAHFP) supporting electrolyte with different scan rates.

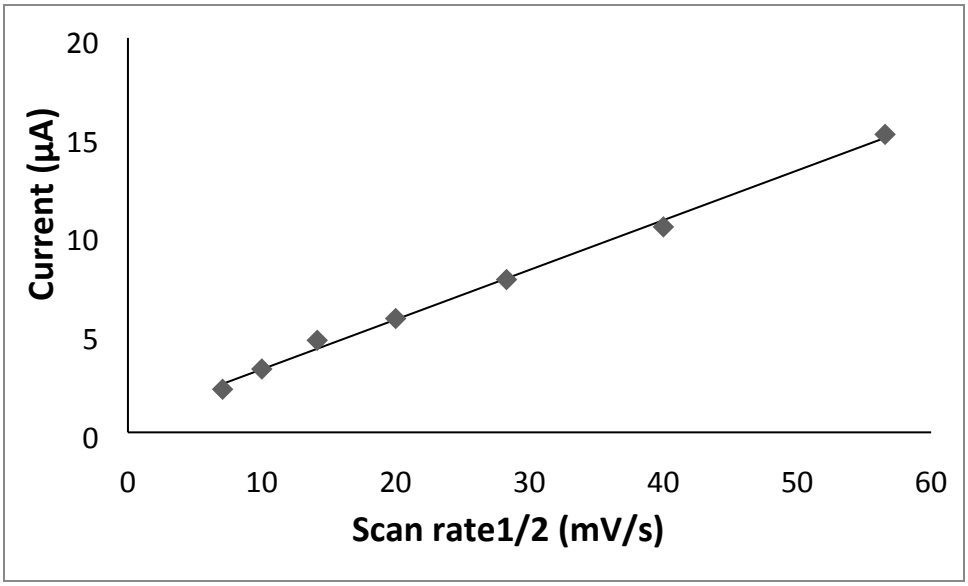

Figure S6. Plot of scan rate$^{1/2}$ vs current for the first reduction peak of [Mn(κ^3-tpa)$(CO)_3$]OTf

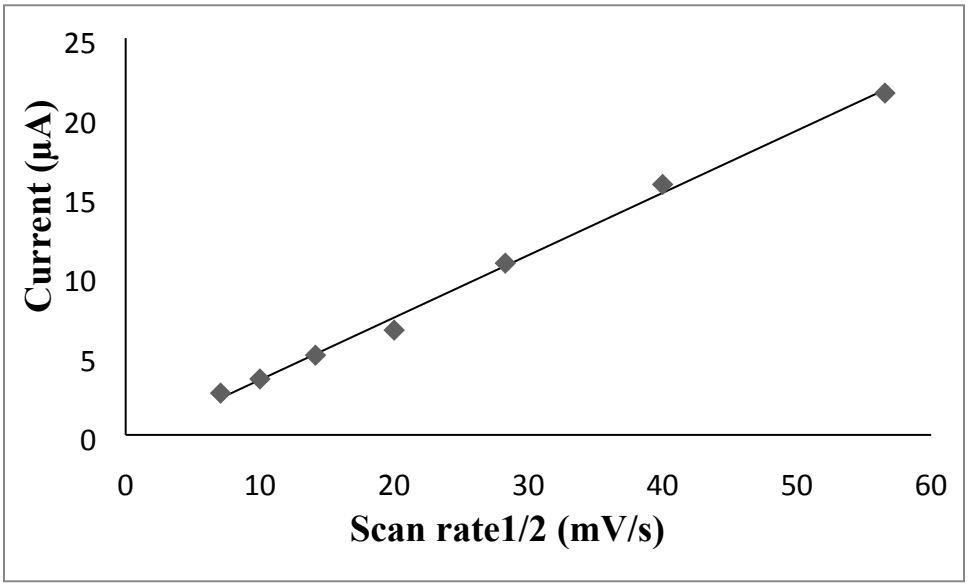

Figure S7. Plot of scan rate$^{1/2}$ vs current for the second reduction peak of [Mn(κ^3-tpa)$(CO)_3$]OTf

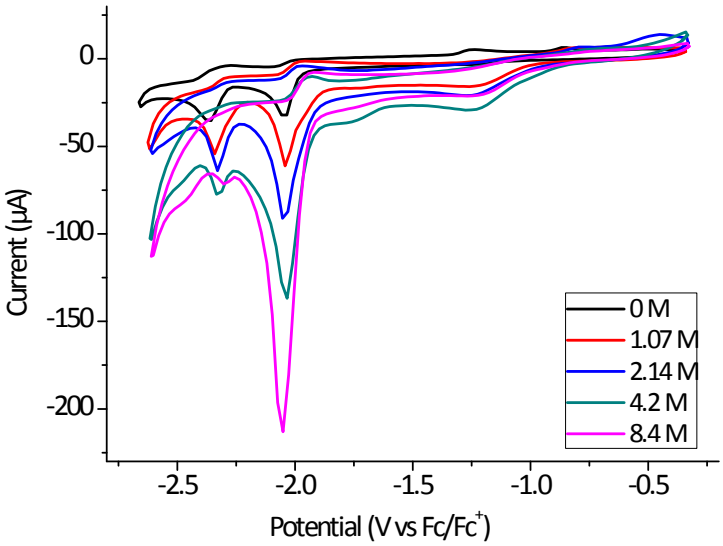

Figure S8. Cyclic voltammogram of [Mn(κ^3-tpa)$(CO)_3$]OTf under $N_2$with increasing concentration of water in 15 mL of CH_3CN with 0.1M tetrabutylammoniumhexafluorophosphate (TBAHFP) supporting electrolyte at 100 mV/s.

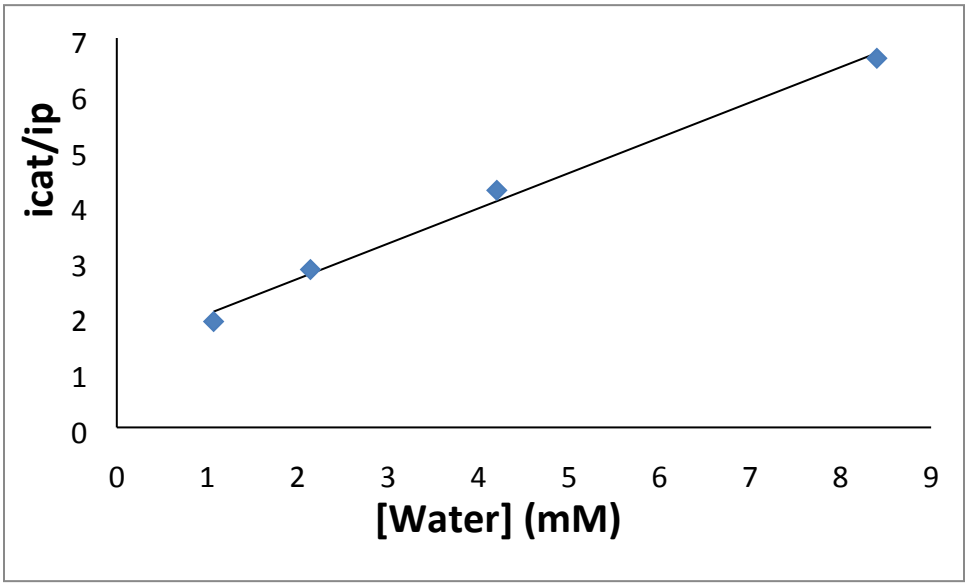

Figure S9. Plot of i_{cat}/i_p versus increasing concentration of water in CH_3CN for the electrocatalytic reduction of water using [Mn(κ^3-tpa)$(CO)_3$]OTf with 0.1M tetrabutylammoniumhexafluorophosphate (TBAHFP) supporting electrolyte at 100 mV/s. Turn over frequencies estimated using the equation $TOF = \frac{Fvn_p{}^3}{RT}\left(\frac{0.4463}{n_{cat}}\right)^2\left(\frac{i_{cat}}{i_p}\right)^2$ gave a value of 6.8 s^{-1} with 8mM water.

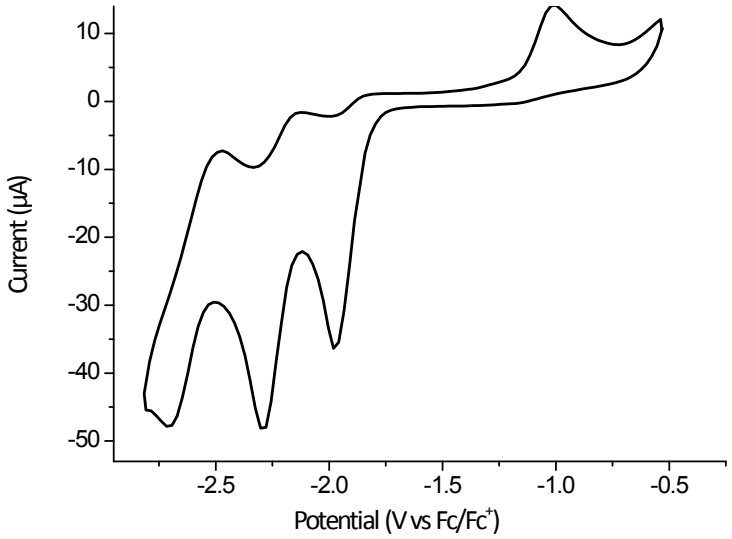

Figure S10. Cyclic voltammogram of [Mn(κ^3-tpa)$(CO)_3$]Br under N_2 in CH_3CN with 0.1M tetrabutylammonium hexafluorophosphate (TBAHFP) as supporting electrolyte at 100 mV/s.

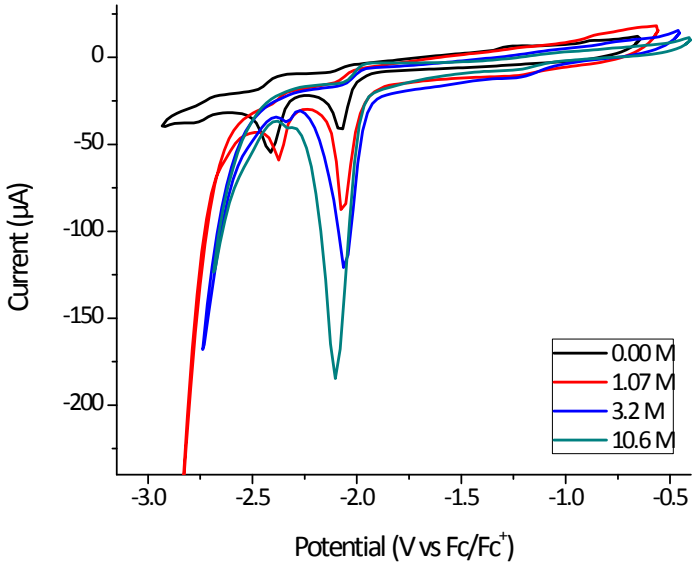

Figure S11. Cyclic voltammogram of [Mn(κ^3-tpa)$(CO)_3$]Br under N_2 and with increasing concentration of water in CH_3CN with 0.1M tetrabutylammonium hexafluorophosphate (TBAHFP) supporting electrolyte at 100 mV/s.

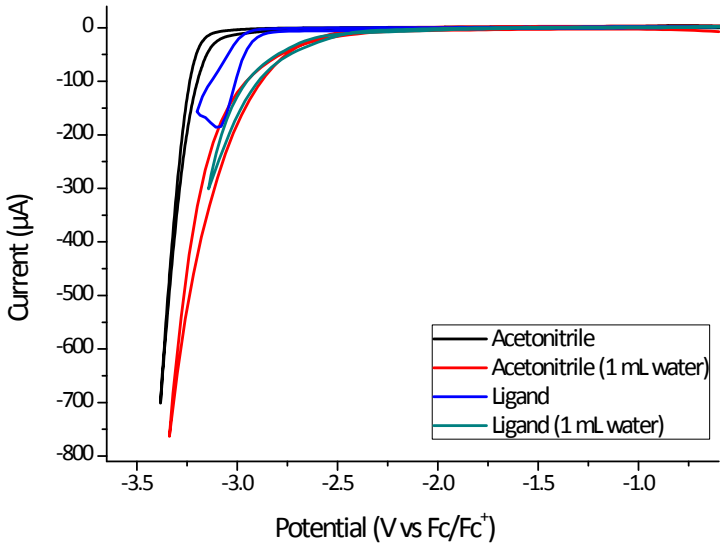

Figure S12. Cyclic voltammograms for acetonitrile and tpa ligand using a glassy carbon working electrode under N_2 with 0.1M tetrabutylammoniumhexafluorophosphate (TBAHFP) supporting electrolyte at 100 mV/s (black and blue traces respectively). Under the same conditions these measurements were also carried out with addition of 1mL of water (red and green traces respectively).

Table S3. Bulk electrolysis at the potential of the first reduction peak for [Mn(κ^3-tpa)$(CO)_3$]OTf. Catalyst concentration of 1mM and 100mM supporting electrolyte in 15mL acetonitrile with addition of 2 mL water.

Time (s)	µmol of H_2 (Theoretical)	µmol of H_2 (Obtained)
0	0	0
2000	19	13
6000	52	25
11000	100	33

Table S4. Bulk electrolysis at the potential of the first reduction peak for [Mn(κ^3-tpa)$(CO)_3$]Br. Catalyst concentration of 1mM and 100mM supporting electrolyte in 15mL acetonitrile with addition of 2 mL water.

Time (s)	µmol of H_2 (Theoretical)	µmol of H_2 (Obtained)
0	0	0
3600	19	16
7200	52	23
11000	78	30
56750	284	123

Table S5. Bulk electrolysis experiments in presence of 1.5 mL phosphate buffer (pH 7) at first reduction peak of [Mn(κ^3-tpa)(CO)$_3$]OTf.

Time (s)	µmol of H_2 (theoretical)	µmol of H_2 (Obtained)
0	0	0
1800	47	23
3800	107	44
7200	195	62

Table S6. Bulk electrolysis experiments in presence of 1.5 mL phosphate buffer (pH 7) at first reduction peak of [Mn(κ^3-tpa)(CO)$_3$]Br.

Time (s)	µmol of H_2 (theoretical)	µmol of H_2 (Obtained)
0	0	0
1800	71	38
4200	188	91
7400	358	137

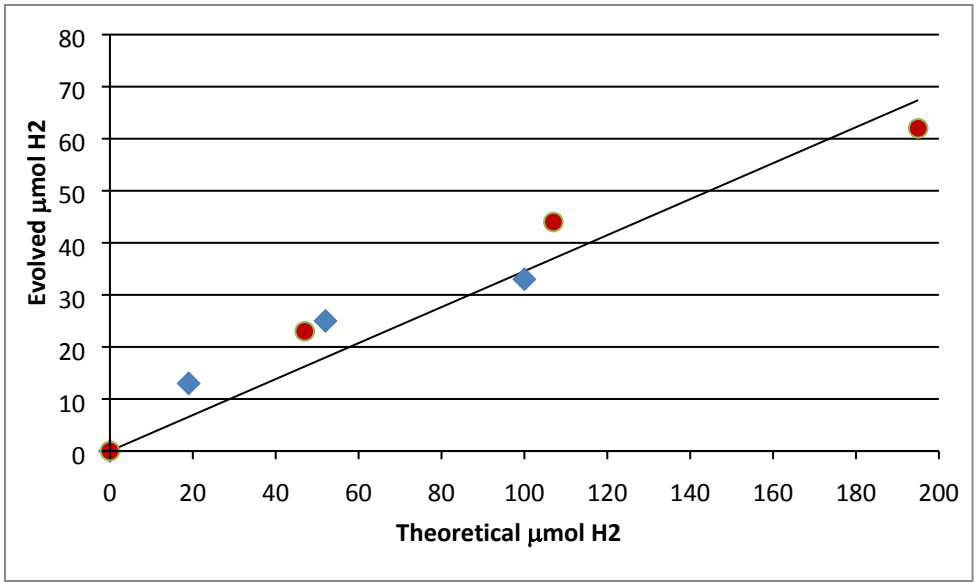

Figure S13. Controlled potential electrocatalytic production of H_2 in acetonitrile at −2.0 V by 1.0mM [Mn(tpa)(CO)$_3$]OTf (**1**$^+$OTf$^-$) from H_2O (183 min., blue diamonds) and from aqueous phosphate buffer (120 min., red circles). The line represents a linear regression of this data and indicates 35% efficiency.

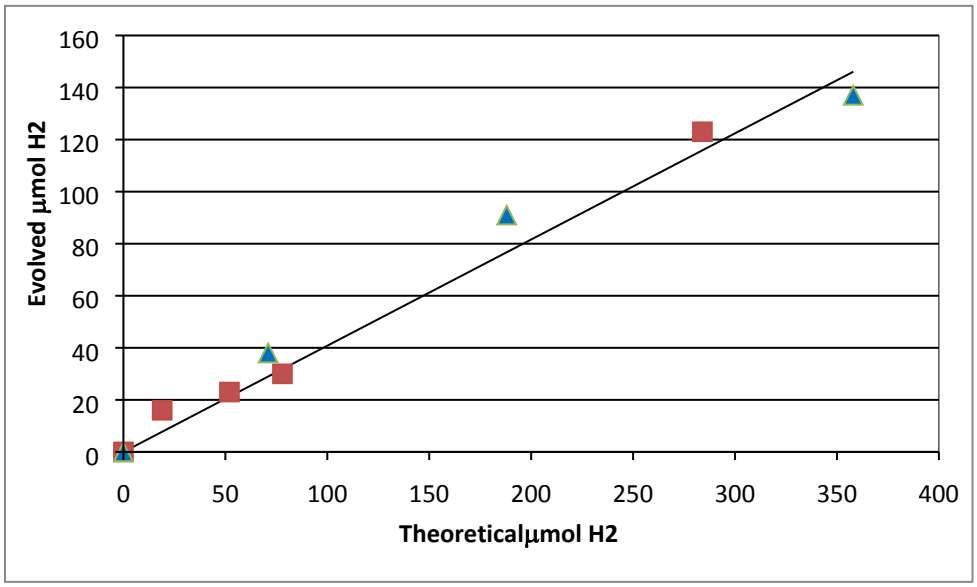

Figure S14. Controlled potential electrocatalytic production of H_2 in acetonitrile at −2.0 Vby 1.0mM [Mn(tpa)(CO)$_3$]Br (**1**$^+$Br$^-$) from H_2O (945 min., blue triangles) and from aqueous phosphate buffer (120 min., red squares).The line represents a linear regression of this data and indicates 41% efficiency.

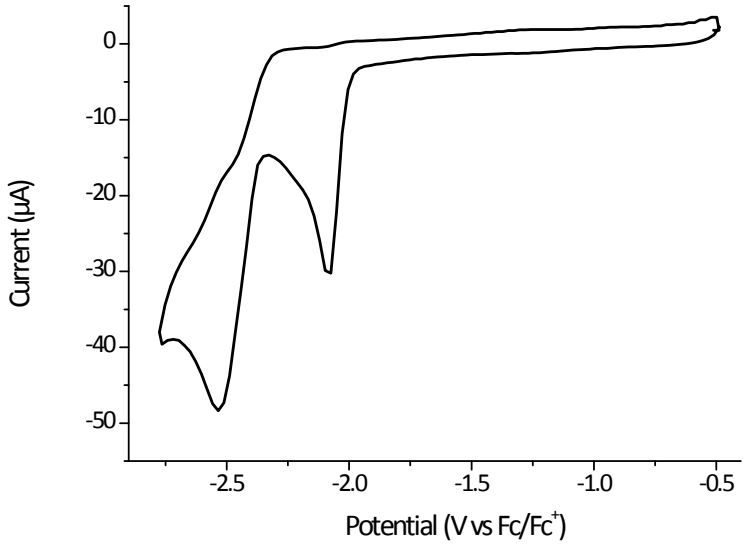

Figure S15. Cyclic voltammogram of [Re(κ^3-tpa)(CO)$_3$]OTf in CH_3CN with 0.1M tetrabutylammoniumhexafluorophosphate (TBAHFP) supporting electrolyte.

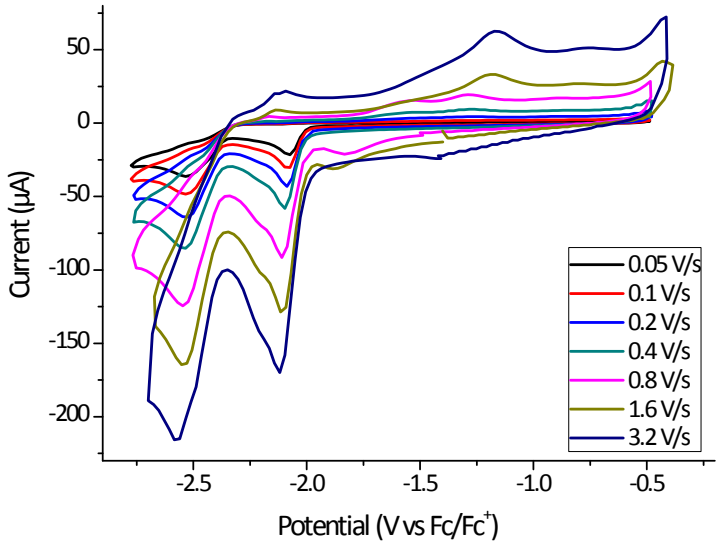

Figure S16. Cyclic voltammogram of [Re(κ^3-tpa)(CO)$_3$]OTf in CH_3CN with 0.1M tetrabutylammoniumhexafluorophosphate (TBAHFP) supporting electrolyte with different scan rate.

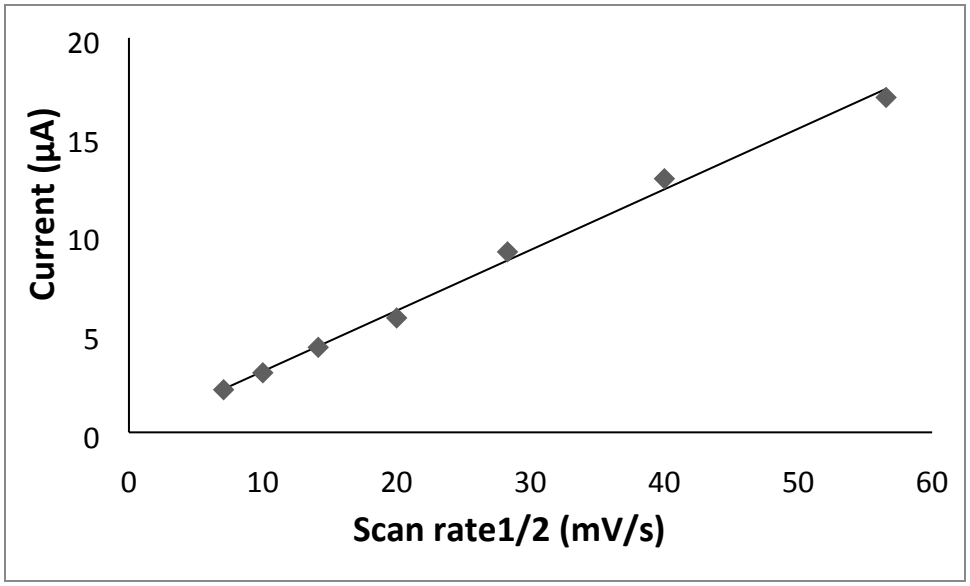

Figure S17. Plot of scan rate$^{1/2}$ vs current at first reduction peak of [Re(κ^3-tpa)(CO)$_3$]OTf in CH_3CN.

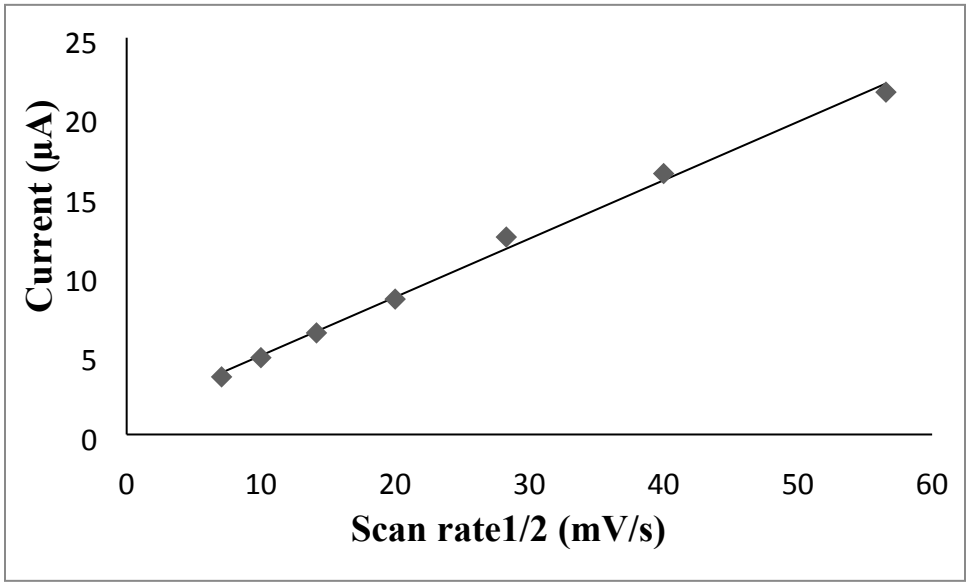

Figure S18. Plot of scan rate$^{1/2}$ vs current at second reduction peak of [Re(κ^3-tpa)(CO)$_3$]OTf in CH_3CN.

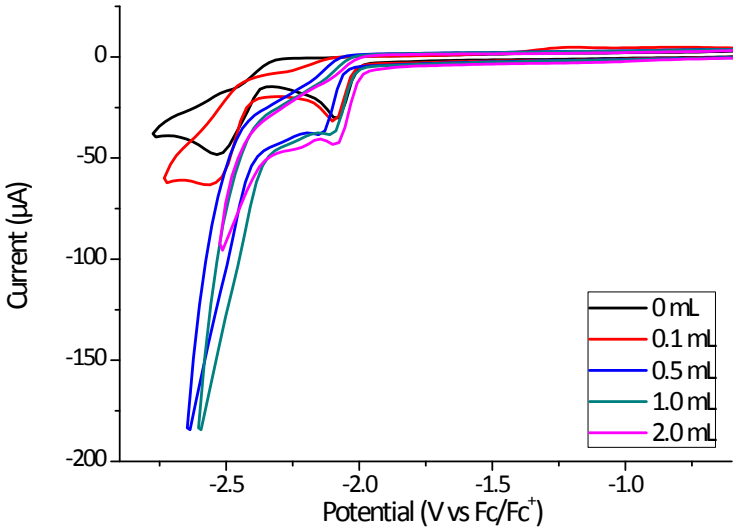

Figure S19. Cyclic voltammogram of [Re(κ^3-tpa)$(CO)_3$]OTf under N_2 and increasing concentration of water in CH_3CN with 0.1M tetrabutylammoniumhexafluorophosphate (TBAHFP) supporting electrolyte at 100 mV/s.

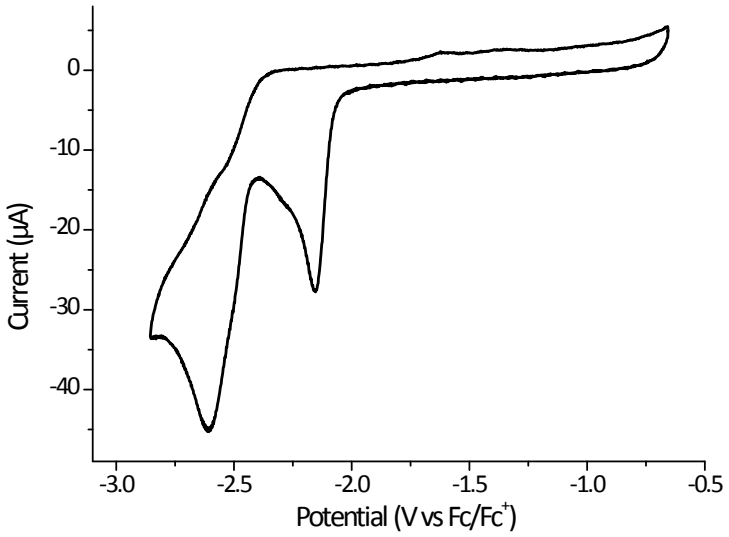

Figure S20. Cyclic voltammogram of [Re(κ^3-tpa)(CO)$_3$]Br under N_2 in CH_3CN with 0.1M tetrabutylammoniumhexafluorophosphate (TBAHFP) supporting electrolyte at 100 mV/s.

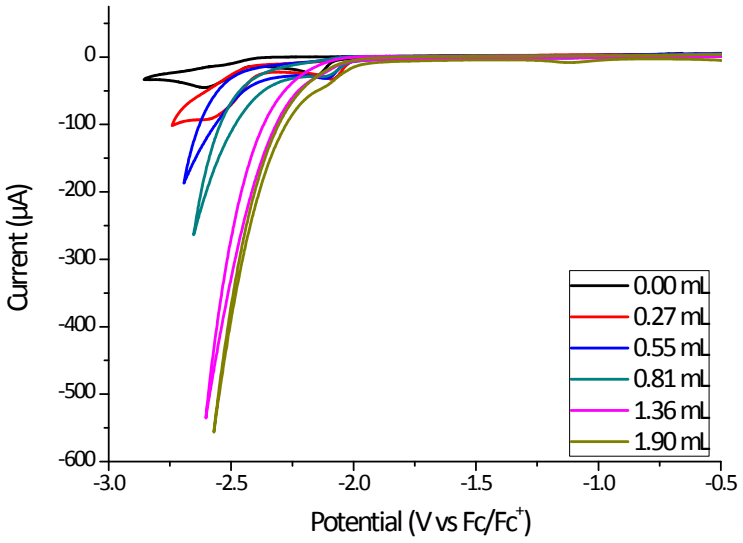

Figure S21. Cyclic voltammogram of [Re(κ^3-tpa)(CO)$_3$]Br under N_2 and increasing concentration of water in CH_3CN with 0.1M tetrabutylammoniumhexafluorophosphate (TBAHFP) supporting electrolyte at 100 mV/s.

Table S7. Bulk electrolysis experiments in presence of 1.5 mL water at first reduction peak of [Re(κ^3-tpa)$(CO)_3$]OTf.

Time (s)	µmol of H_2 (Calculated)	µmol of H_2 (Obtained)
0	0	0
3600	38	17
8100	69	40

Table S8. Bulk electrolysis experiments in presence of 1.5 mL phosphate buffer (pH 7) at first reduction peak of [Re(κ^3-tpa)$(CO)_3$]OTf.

Time (s)	µmol of H_2 (Calculated)	µmol of H_2 (Obtained)
0	0	0
1800	38	13
8000	639	179
13000	1154	371

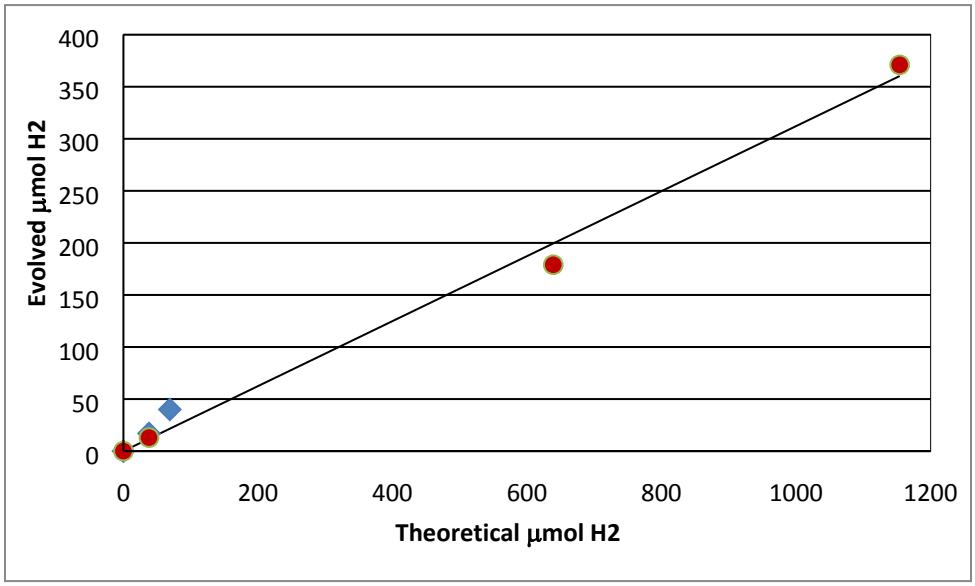

Figure S22. Controlled potential electrocatalytic production of H_2 in acetonitrile at −2.0 V by 1.0mM [Re(tpa)$(CO)_3$]OTf (**2**$^+$OTf$^-$) from H_2O (135 min., blue diamonds) and from aqueous phosphate buffer (216 min., red circles). The line represents a linear regression of this data and indicates 31% efficiency.

Table S9. A comparison of metal –ligand distances in the computationally optimized structures of the parent cation $[Mn(CO)_3(\kappa^3\text{-tpa})]^+$(**1**$^+$) and that of the single electron reduction product $[Mn(CO)_3(\kappa^3\text{-tpa})]$ (**1**) and the double reduction product $[Mn(CO)_3(\kappa^3\text{-tpa})]^-$ (**1**$^-$)

Bond/cmpd	$[Mn(CO)_3(\kappa^3\text{-tpa})]^+$(**1**$^+$)	$[Mn(CO)_3(\kappa^3\text{-tpa})]$ (**1**)	$[Mn(CO)_3(\kappa^3\text{-tpa})]^-$(**1**$^-$)
M-N_{amine}	2.192	2.234	2.437
M-N_{py}	2.096	2.095	2.126
M-N_{py}	2.106	2.108	2.108
M-CO equatorial	1.847, 1.837	1.826, 1.818	1.808, 1.806
M-CO axial	1.827	1.811	1.782

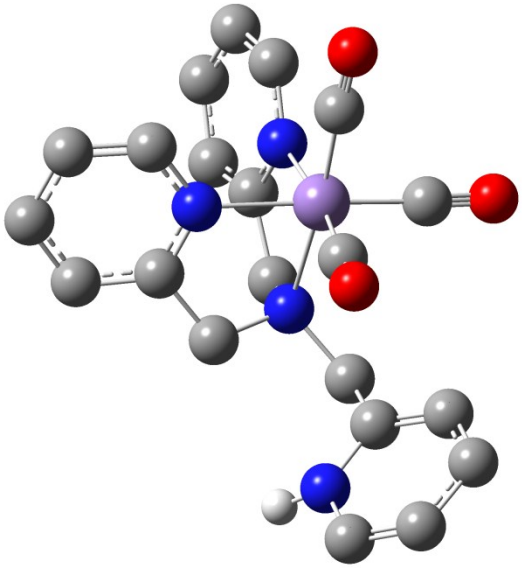

Figure S23. A ball and stick representation of the optimized single reduction product, **1**, with addition of a proton, $[Mn(\kappa^3\text{-tpaH})(CO)_3]^+$(**1H**) in CH_3CN. This species is discussed in the text. For clarity, only the added proton is shown.

Table S10. Optimized coordinates for single reduction product, **1**, with added proton [Mn(κ^3-tpaH)$(CO)_3]^+$(**1H**) as discussed in the text.

Standard orientation:

Center Number	Atomic Number	Atomic Type	Coordinates (Angstroms) X	Y	Z
1	25	0	0.318347	-0.732685	0.663983
2	8	0	1.478625	-1.798842	3.179807
3	8	0	-2.029298	-0.042995	2.369039
4	8	0	-0.607830	-3.490261	0.032082
5	6	0	1.057875	-1.374445	2.199727
6	6	0	-1.177718	-0.311387	1.651686
7	6	0	-0.268051	-2.420058	0.263250
8	7	0	-0.398125	0.151221	-1.199307
9	7	0	2.058638	-0.960045	-0.479746
10	7	0	1.058203	1.219893	0.890694
11	7	0	-3.625725	1.152384	-1.157385
12	6	0	0.628980	-0.130072	-2.251926
13	1	0	0.673354	0.688682	-2.973481
14	1	0	0.297359	-1.012493	-2.803843
15	6	0	1.994081	-0.447856	-1.720526
16	6	0	3.121945	-0.321686	-2.524673
17	1	0	3.029900	0.109748	-3.512248
18	6	0	4.346319	-0.764286	-2.048716
19	1	0	5.235947	-0.678242	-2.658650
20	6	0	4.406972	-1.322931	-0.777394
21	1	0	5.335793	-1.690090	-0.363914
22	6	0	3.248019	-1.393897	-0.025301
23	1	0	3.266985	-1.807587	0.971984
24	6	0	-0.479117	1.611770	-0.920782
25	1	0	-1.411056	1.787872	-0.382747
26	1	0	-0.519073	2.185627	-1.850882
27	6	0	0.637002	2.091504	-0.044235
28	6	0	1.145071	3.381625	-0.130109
29	1	0	0.789247	4.048472	-0.903577
30	6	0	2.101446	3.793471	0.786944
31	1	0	2.510206	4.794311	0.741084
32	6	0	2.522962	2.898601	1.762652
33	1	0	3.264008	3.173355	2.500079
34	6	0	1.984536	1.623043	1.775967
35	1	0	2.301481	0.899967	2.513207
36	6	0	-1.729818	-0.318016	-1.808478
37	1	0	-1.805510	0.169369	-2.788686
38	1	0	-1.608551	-1.383485	-1.985040
39	6	0	-2.989983	-0.102347	-1.049769
40	6	0	-3.646290	-1.095462	-0.354865
41	1	0	-3.175066	-2.067950	-0.291077
42	6	0	-4.886181	-0.884346	0.256344
43	1	0	-5.380203	-1.678875	0.796135

44	6	0	-5.493501	0.399353	0.119594
45	1	0	-6.456234	0.608689	0.566125
46	6	0	-4.874093	1.374013	-0.591953
47	1	0	-5.292120	2.356684	-0.752992
48	1	0	-3.300793	1.806121	-1.852889

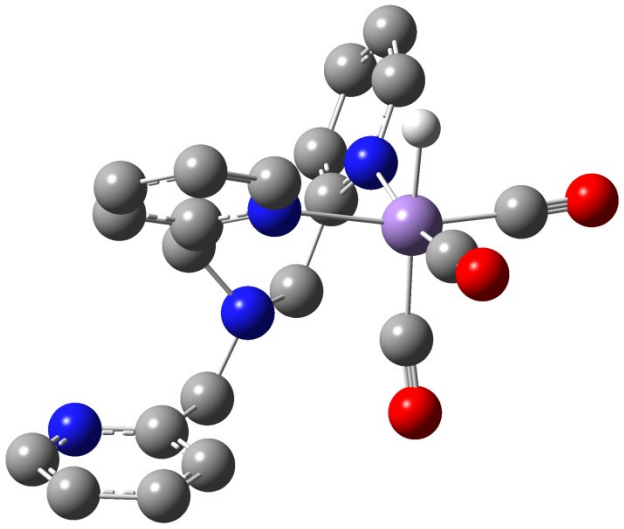

Figure S24. A ball and stick representation of the optimized double reduction product of, **1**$^{-}$, with addition of a proton in CH_3CN, [MnH(κ^2-tpa)$(CO)_3$](**1**$^{-}$**H**) as discussed in the text. For clarity, only the added proton is shown.

Table S11. Optimized coordinates for double reduction product, **1**$^{-}$, with added proton [MnH(κ^2-tpa)(CO)$_3$] (**1**$^{-}$**H**) as discussed in the text.

Standard orientation:

Center Number	Atomic Number	Atomic Type	Coordinates (Angstroms) X	Y	Z
1	25	0	-1.470054	1.223786	-0.276896
2	8	0	-4.017799	1.788185	-1.637562
3	8	0	-0.753231	4.045184	-0.721933
4	8	0	-0.110840	0.591850	-2.858018
5	6	0	-3.004990	1.554674	-1.130405
6	6	0	-0.996776	2.927480	-0.545810
7	6	0	-0.589631	0.716424	-1.813017
8	7	0	0.439192	-1.498605	-0.557791
9	7	0	-2.336846	-0.736059	0.295753
10	7	0	0.224457	0.915011	1.225520
11	7	0	3.802012	-1.869803	-0.357320
12	6	0	-0.771744	-2.187990	-1.002816
13	1	0	-0.613222	-3.275223	-1.055750
14	1	0	-0.988086	-1.864003	-2.025942
15	6	0	-1.997744	-1.968504	-0.144958
16	6	0	-2.764414	-3.091691	0.173084
17	1	0	-2.451545	-4.060638	-0.191615
18	6	0	-3.901433	-2.970157	0.954595
19	1	0	-4.499602	-3.838561	1.199120
20	6	0	-4.234132	-1.710259	1.428643
21	1	0	-5.097116	-1.547361	2.059717
22	6	0	-3.430352	-0.638586	1.080371
23	1	0	-3.655008	0.355429	1.433337
24	6	0	0.668797	-1.519191	0.881878
25	1	0	1.480995	-2.204101	1.142589
26	1	0	-0.214915	-1.903804	1.392829
27	6	0	0.980389	-0.169881	1.501390
28	6	0	2.015402	-0.124343	2.439439
29	1	0	2.598799	-1.018003	2.615956
30	6	0	2.291713	1.043228	3.128493
31	1	0	3.095397	1.084407	3.852676
32	6	0	1.502064	2.152977	2.863788
33	1	0	1.652202	3.095761	3.372022
34	6	0	0.495753	2.038170	1.921027
35	1	0	-0.141426	2.884136	1.720462
36	6	0	1.587591	-1.950731	-1.354916
37	1	0	1.779630	-3.022552	-1.196334
38	1	0	1.322612	-1.814961	-2.406322
39	6	0	2.877573	-1.211307	-1.070330
40	6	0	3.097637	0.080909	-1.552136
41	1	0	2.333983	0.576378	-2.135161
42	6	0	4.304091	0.709577	-1.277868

43	1	0	4.496932	1.710572	-1.643440
44	6	0	5.261278	0.029236	-0.532967
45	1	0	6.217508	0.477597	-0.297345
46	6	0	4.962271	-1.255976	-0.099697
47	1	0	5.684279	-1.822708	0.478916
48	1	0	-2.216867	1.793088	1.016913

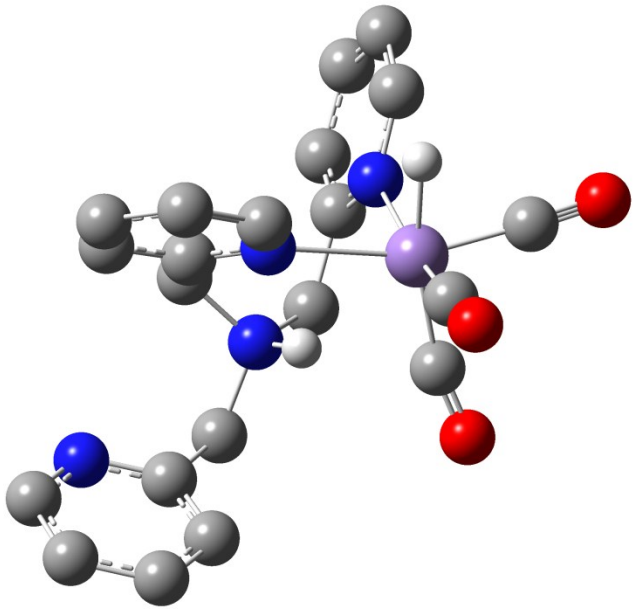

Figure S25.A ball and stick representation of the optimized double reduction product of **1**$^{+}$with addition of a second proton in CH_3CN, $[MnH(\kappa^2\text{-tpaH})(CO)_3]^{+}$(**1**$^{-}$**HH**$^{+}$) as discussed in the text. For clarity, only the added protons are shown.

Table S12. Optimized coordinates for double reduction product with two added protons, [MnH(κ^2-tpaH)$(CO)_3$]$^+$ (**1**$^-$**HH**$^+$),as discussed in the text.

Standard orientation:

Center Number	Atomic Number	Atomic Type	Coordinates (Angstroms) X	Y	Z
1	25	0	-1.479895	1.214788	-0.204213
2	8	0	-4.116413	1.985176	-1.265881
3	8	0	-0.679059	4.058184	-0.242048
4	8	0	-0.508181	1.196436	-3.012833
5	6	0	-3.074800	1.677734	-0.888288
6	6	0	-0.961417	2.942945	-0.227369
7	6	0	-0.791446	1.055791	-1.897929
8	7	0	0.517185	-1.359223	-0.750247
9	7	0	-2.293851	-0.796499	0.153740
10	7	0	0.184356	0.694729	1.331851
11	7	0	3.735141	-1.597606	-0.307698
12	6	0	-0.718839	-2.024770	-1.318035
13	1	0	-0.463043	-3.062278	-1.515064
14	1	0	-0.919858	-1.536222	-2.270317
15	6	0	-1.917669	-1.968004	-0.407608
16	6	0	-2.606326	-3.155889	-0.181446
17	1	0	-2.258123	-4.068907	-0.644340
18	6	0	-3.723672	-3.162744	0.640321
19	1	0	-4.271150	-4.078679	0.818636
20	6	0	-4.100386	-1.971236	1.237534
21	1	0	-4.950530	-1.912467	1.902817
22	6	0	-3.362810	-0.828078	0.975121
23	1	0	-3.626399	0.111722	1.432862
24	6	0	0.752406	-1.650868	0.709146
25	1	0	1.638037	-2.273995	0.784102
26	1	0	-0.094543	-2.222782	1.080638
27	6	0	0.934326	-0.407295	1.546115
28	6	0	1.854390	-0.498442	2.589127
29	1	0	2.439234	-1.400895	2.700986
30	6	0	2.013498	0.559881	3.466514
31	1	0	2.721832	0.500798	4.282260
32	6	0	1.240069	1.692302	3.263053
33	1	0	1.310046	2.554327	3.911771
34	6	0	0.355739	1.714447	2.199655
35	1	0	-0.262665	2.581936	2.045249
36	6	0	1.718040	-1.675576	-1.636078
37	1	0	1.858359	-2.752513	-1.581095
38	1	0	1.425687	-1.402105	-2.647470
39	6	0	2.986087	-0.969775	-1.225509
40	6	0	3.364022	0.237635	-1.807581
41	1	0	2.743148	0.706568	-2.559522
42	6	0	4.561699	0.823176	-1.411416

43	1	0	4.883554	1.759577	-1.848389
44	6	0	5.336422	0.181090	-0.455899
45	1	0	6.277309	0.597512	-0.121859
46	6	0	4.881102	-1.026486	0.065670
47	1	0	5.462707	-1.559918	0.809040
48	1	0	-2.244825	1.651225	1.109266
49	1	0	0.315387	-0.345813	-0.822262

Table S13. Sum of electronic and thermal free energies corrected for ZPE for the complexes presented in the proposed mechanism (Figure 4). Values were obtained using DFT with the B3LYP functional and TZVP basis set. Optimizations employed the PCM formalism using acetonitrile as solvent.

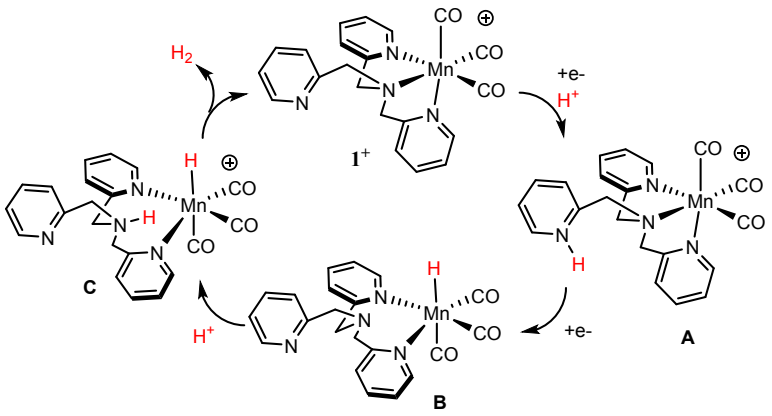

Compound	G(Hartree)
1^{+} $[Mn(\kappa^3\text{-tpa})(CO)_3]^{+}$	-2407.09282083
Addition of a one electron to **1**$^{+}$to yield $[Mn(\kappa^3\text{-tpa})(CO)_3]$ (**1**)	-2407.23369177
Addition of an electron to **1** to yield $[Mn(\kappa^3\text{-tpa})(CO)_3]^{-}$ (**1**$^{-}$)	-2407.25120179
A	-2407.71566735
B (singlet spin state)	-2407.83424702
C	-2408.28022464

For reference the computed free energy of H_2 in the gas phase =-1.187643 Hartree

References

(1) APEX Softward Suite v 2010; Bruker AXS: Madison WI, 2010.
(2) Blessing, B. Y. R. H. *Acta Crystallogr. Sect. A***1995**, 33–38.
(3) Sheldrick, G. M. *Acta Crystallogr. Sect. A***2008**, 112–122.
(4) Frisch, M. J.; Trucks, G. W.; Schlegel, H. B.; Scuseria, G. E.; Robb, M. A.; Cheeseman, J. R.; Scalmani, G.; Barone, V.; Mennucci, B.; Petersson, G. A.; Nakatsuji, H.; Caricato, M.; Li, X.; Hratchian, H. P.; Izmaylov, A. F.; Bloino, J.; Zheng, G.; Sonnenb, D. J. Gaussian 09, Revision A.02.